Decoupling and Damping: Structurally-Regularized Gradient Matching for Multimodal Graph Condensation

Lian Shen Xiamen University Xiamen, China shenlian@stu.xmu.edu.cn

Meijia Song Xiamen University Xiamen, China songmj@stu.xmu.edu.cn Zhendan Chen Xiamen University Xiamen, China chenzhendan@stu.xmu.edu.cn

Ziming Su Xiamen University Xiamen, China suziming@stu.xmu.edu.cn

> Xiangrong Liu Xiamen University Xiamen, China xrliu@xmu.edu.cn

yinhui jiang Xiamen University Xiamen, China stardjyeah@gmail.com

Juan Liu Xiamen University Xiamen, China cecyliu@xmu.edu.cn

Abstract

In critical web applications such as e-commerce and recommendation systems, multimodal graphs integrating rich visual and textual attributes are increasingly central, yet their large scale introduces substantial computational burdens for training Graph Neural Networks (GNNs). While Graph Condensation (GC) offers a promising solution by synthesizing smaller datasets, existing methods falter in the multimodal setting. We identify a dual challenge causing this failure: (1) conflicting gradients arising from semantic misalignments between modalities, and (2) the GNN's messagepassing architecture pathologically amplifying this gradient noise across the graph structure. To address this, we propose Structurally-Regularized Gradient Matching (SR-GM), a novel condensation framework tailored for multimodal graphs. SR-GM introduces two synergistic components: first, a gradient decoupling mechanism that resolves inter-modality conflicts at their source via orthogonal projection; and second, a structural damping regularizer that acts directly on the gradient field. By leveraging the graph's Dirichlet energy, this regularizer transforms the topology from a noise amplifier into a stabilizing force during optimization. Extensive experiments demonstrate that SR-GM significantly improves accuracy and accelerates convergence compared to baseline methods. Ablation studies confirm that addressing both gradient conflict and structural amplification in tandem is essential for achieving superior performance. Moreover, the condensed multimodal graphs exhibit strong cross-architecture generalization and promise to accelerate

applications like Neural Architecture Search. This research provides a scalable methodology for multimodal graph-based learning in resource-constrained environments.

CCS Concepts

• Information systems \to Data mining; • Theory of computation \to Graph algorithms analysis.

Keywords

Multimodal Graph Condensation, Decoupled Gradient Matching, Structural Regularization

ACM Reference Format:

1 Introduction

The deep integration of the Internet and multimedia technologies has spawned a massive amount of graph-structured data containing rich heterogeneous information. From users in social networks and the multimedia content they publish [14, 28, 30, 31, 38] to product graphs associated with text descriptions and product images on e-commerce platforms [3, 43], these multimodal graphs have become the core of modern web applications. Graph neural networks (GNNs) [15, 27, 47], as powerful tools for processing such data, have achieved remarkable results in tasks such as node classification and link prediction. However, their success relies heavily on large-scale datasets [28, 35], which leads to high computational costs, including lengthy training time, huge memory consumption, and complex hyperparameter tuning [1, 49].

To address this challenge, a data-centric approach, dataset condensation [39, 51], has emerged. Its goal is to refine the original large-scale dataset into a small synthetic dataset with highly concentrated information, so that the model trained on this synthetic dataset can achieve performance comparable to that trained on the

Permission to make digital or hard copies of all or part of this work for personal or classroom use is granted without fee provided that copies are not made or distributed for profit or commercial advantage and that copies bear this notice and the full citation on the first page. Copyrights for components of this work owned by others than the author(s) must be honored. Abstracting with credit is permitted. To copy otherwise, or republish, to post on servers or to redistribute to lists, requires prior specific permission and/or a fee. Request permissions from permissions@acm.org.

Conference'17, Washington, DC, USA

© 2025 Copyright held by the owner/author(s). Publication rights licensed to ACM. ACM ISBN 978-x-xxxx-xxxx-x/YYYY/MM

https://doi.org/10.1145/nnnnnn.nnnnnnn

full dataset. In the field of computer vision, gradient matching [51] has become a benchmark method for achieving this goal. It efficiently learns highly representative synthetic samples by matching the model's training gradient trajectories on real data and synthetic data. Recently, researchers have begun to extend this paradigm to graph-structured data and proposed a variety of graph condensation methods [8, 13, 19]. These methods are usually formulated as a complex bi-level optimization problem, aiming to learn a miniature synthetic graph structure and its node features through objectives such as gradient matching [13] or distribution matching [19].

Although these methods show potential on unimodal graphs (with node features from a unimodal source), their performance degrades significantly when directly applied to more general multimodal graphs (where nodes have multiple modal features such as text and images). Through in-depth analysis, we find that the root cause lies in the conflict between multimodal gradient signals and the pathological amplification effect of the graph structure on this conflict. Specifically, there may be a semantic gap between different modalities (such as text and image) [17, 48], which leads to the generation of gradients in opposite directions during the optimization process. More importantly, the inherent message passing mechanism of GNN will quickly propagate and amplify the gradient conflicts of these local nodes to the entire graph, thus making the optimization process of the condensation algorithm based on gradient matching unstable and ineffective.

To overcome this problem, this paper proposes a novel structurally regularized gradient matching (SR-GM) framework designed for multimodal graph condensation. The core ideas of SR-GM are twofold: (1) Gradient decoupling: At its core, we adopt the idea of conflict disentanglement from multi-task learning [2, 46]. Specifically, for the conflicting gradients arising from different modalities on a synthetic node, we apply orthogonal projection to eliminate their inherent contradictions, thereby achieving synergistic inter-modal gradient collaboration; (2) Structural damping: On the propagation path, we innovatively introduce a graph Laplacian regularization term that acts on the gradient field rather than node features. This regularization term forces the optimization directions of adjacent nodes to be consistent during the condensation process, thereby transforming the graph structure from a "conflict amplifier" to an "optimization damper", effectively suppressing the spread of gradient noise.

We conducted extensive experiments on multiple multimodal graph benchmark datasets. Our results demonstrate that SR-GM significantly outperforms existing graph condensation baselines. Detailed ablation studies confirm the necessity and effectiveness of the two components, gradient decoupling and structural damping. Furthermore, the condensed graphs generated by SR-GM exhibit excellent generalization across diverse GNN architectures, highlighting its robustness and practicality.

The main contributions of this paper are as follows:

 We provide the first in-depth analysis of the mechanisms of gradient conflict in multimodal graph condensation and its negative effects amplified by graph structure, providing a novel theoretical perspective for understanding the underlying problem.

- We propose the SR-GM method, which systematically addresses the core challenges of multimodal graph condensation through the dual design of gradient decoupling and structural damping.
- We validate the superior performance of SR-GM through rigorous experiments and demonstrate the strong generalization of the generated condensed data in cross-architecture evaluations.

2 Related Work

2.1 Graph Dataset Condensation

Dataset Condensation (DC), also known as Dataset Distillation, aims to synthesize a small, informative dataset from a large original one such that models trained on the synthetic set achieve performance comparable to those trained on the original data. This paradigm was first pioneered in the image domain, where methods were developed to optimize synthetic pixels directly through a bi-level optimization framework [39]. The core idea is to match certain properties between the real and synthetic data. Various matching criteria have been proposed, including matching model performance [51] and feature distributions [36, 50]. Among these, matching the gradients of model parameters has been proven to be a particularly effective strategy [51]. The extension of these techniques to the graph domain, termed Graph Condensation (GC), is a nascent and challenging endeavor. Jin et al. [13] first extended DC to graphs, introducing a node-level condensation method. Unlike image data, graph data involves an intricate coupling between node attributes and topological structure, making the joint synthesis of features and edges a complex optimization task. Current GC methods primarily focus on preserving information in singlemodal graphs, exploring strategies such as gradient matching [13], training trajectory matching [52], and distribution matching [19]. Recent research has evolved from developing efficient and interpretable graph condensation methods [5, 37] to creating specialized techniques tailored for specific graph types, such as heterogeneous graphs and signed graphs [9, 16]. However, these methods largely overlook the unique challenges posed by multimodal graphs, where node features themselves are composed of heterogeneous information from sources like text and images. The problem of inter-modal signal conflict within the GC framework remains a critical and underexplored gap. Our work aims to bridge this gap.

2.2 Multimodal Graph Learning

Multimodal Graph Learning (MGL) has emerged as a vital field for analyzing complex real-world systems where entities are described by multiple data types (e.g., text, images, audio). MGL aims to leverage the relational structure of graphs to fully explore associations both within and between different modalities. This is particularly challenging because data fusion must be guided by the graph topology, which itself may vary across modalities. A key challenge in MGL is bridging the "semantic gap", where different modalities may provide conflicting or inconsistent representations of the same entity [17, 54]. For instance, two products might be visually similar but have different textual descriptions, creating discrepancies that unimodal models cannot resolve. To address this, significant research

has focused on feature alignment, which aims to map representations from different modalities into a unified embedding space. Contrastive learning frameworks, such as CLIP [25], have been notably successful in learning aligned vision-language representations. From an architectural perspective, methods like Multimodal Graph Convolutional Networks (MGCN) [41] and Multimodal Graph Attention Networks (MGAT) [31] have been proposed to explicitly model and fuse information from different modalities. While these MGL methods focus on designing more sophisticated Graph Neural Network (GNN) architectures to better handle existing multimodal data, they do not address the data-centric challenge of scalability [1, 24]. The question of how to effectively compress large-scale multimodal graphs, particularly in a way that handles the feature conflicts inherent in the condensation process, remains largely unaddressed. Our work bridges this gap by introducing a condensation method specifically designed with an optimization scheme attuned to the uniqueness of multimodal graphs.

3 Methodology

3.1 Problem Formulation

We consider the problem of multimodal graph condensation, where the objective is to distill a large-scale multimodal graph into a compact yet informative synthetic graph while preserving the essential information for downstream tasks.

Let the large-scale original graph be denoted as $\mathcal{T}=(\mathbf{X},\mathbf{A},\mathbf{Y})$, where $\mathbf{X}\in\mathbb{R}^{N\times d}$ is the node feature matrix for N nodes, $\mathbf{A}\in\mathbb{R}^{N\times N}$ is the adjacency matrix, and $\mathbf{Y}\in\{0,1,\ldots,C-1\}^N$ are the node labels over C classes. In the context of multimodal graphs, the d-dimensional feature vector for each node is a concatenation of features from different modalities, i.e., $\mathbf{X}_i=[\mathbf{x}_{i,\text{text}}\oplus\mathbf{x}_{i,\text{image}}]$.

The objective of graph condensation is to synthesize a small, information-rich graph $\mathcal{S}=(\mathbf{X}_{\mathcal{S}},\mathbf{A}_{\mathcal{S}},\mathbf{Y}_{\mathcal{S}})$ with N' nodes $(N'\ll N)$, such that a Graph Neural Network (GNN) model, ϕ_{θ} , trained on \mathcal{S} achieves comparable performance to the same model trained on \mathcal{T} .

3.2 Gradient Matching for Multimodal Graph

This goal is formally captured as a bi-level optimization problem [12]. The outer loop seeks to find the optimal synthetic graph S^* by minimizing a loss $\mathcal{L}_{\text{outer}}$ that evaluates a model trained on S. The inner loop trains this model on S to convergence to obtain the optimal parameters θ_S^* . This can be written as:

$$S^* = \arg\min_{S} \mathcal{L}_{\text{outer}}(\phi_{\theta_{S}^*}, \mathcal{T}) \quad \text{s.t.} \quad \theta_{S}^* = \arg\min_{\theta} \mathcal{L}_{\text{inner}}(\phi_{\theta}, S)$$
(1)

Solving this formulation directly is computationally prohibitive, as it requires fully training a GNN in the inner loop for every single update to the synthetic graph $\mathcal S$ in the outer loop.

The Gradient Matching (GM) paradigm offers an efficient and effective approximation to this problem [13]. Instead of matching the performance of fully converged models, GM aims to align the learning dynamics by matching the parameter gradients at each step of a single training trajectory. The process involves two interleaved optimizations: an outer-loop optimization for the synthetic data $\mathcal S$ and an inner-loop update for the model parameters θ . The objective

is to minimize the cumulative distance between the gradients over the entire trajectory:

$$\min_{\mathcal{S}} \mathbb{E}_{\theta_0 \sim P_{\theta}} \left[\sum_{t=0}^{T-1} D(\nabla_{\theta} \mathcal{L}_{\mathcal{S}}(\theta_t), \nabla_{\theta} \mathcal{L}_{\mathcal{T}}(\theta_t)) \right]$$
(2)

where the model parameters are updated in an inner loop according to the synthetic data: $\theta_{t+1} = \theta_t - \eta_\theta \nabla_\theta \mathcal{L}_{\mathcal{S}}(\theta_t)$. Here, $\mathcal{L}_{\mathcal{S}}$ and $\mathcal{L}_{\mathcal{T}}$ are the task losses, and $D(\cdot, \cdot)$ is a distance metric between the gradient vectors.

Traditional gradient matching methods, while successful in unimodal domains, face significant challenges when applied to multimodal graphs due to two fundamental issues.

3.3 Inter-Modality Gradient Conflict

The outer loop of the GM algorithm is tasked with updating the synthetic graph S to minimize the distance to a target gradient, $g_{\mathcal{T}} = \nabla_{\theta} \mathcal{L}_{\mathcal{T}}$, sampled from the real data. In the multimodal setting, this target gradient becomes inherently unreliable.

To formalize this, we frame the GNN's learning process as a Multi-Task Learning (MTL) problem [18, 40], where each modality constitutes a distinct task being learned by the shared backbone, parameterized by $\theta_{\rm sh}.$ The total gradient $g_{\mathcal T}$ is a linear combination of the gradients from each modality:

$$\nabla_{\theta_{\rm sh}} \mathcal{L}_{\rm total} = \sum_{k \in \{\text{text, image}\}} w_k \nabla_{\theta_{\rm sh}} \mathcal{L}_k \tag{3}$$

This simple summation becomes problematic due to the feature-level "semantic gap" inherent in multimodal data [6, 20]. This misalignment generates opposing update signals, leading to a gradient conflict[21, 22], formally defined as the condition where the gradients of two tasks have a negative cosine similarity:

$$\langle \nabla_{\theta_{sh}} \mathcal{L}_{text}, \nabla_{\theta_{sh}} \mathcal{L}_{image} \rangle < 0$$
 (4)

When this occurs, the target gradient $g_{\mathcal{T}}$ becomes a high-variance and suboptimal signal. It represents a blind compromise between conflicting objectives rather than a stable, Pareto-optimal update direction [22]. Consequently, the outer loop of GM is tasked with matching a noisy, erratically moving target, which fundamentally destabilizes the meta-optimization of \mathcal{S} .

3.4 Structural Amplification of Gradient Noise

The instability is further compounded by the GNN's message-passing mechanism [7], which corrupts the update step of the outer loop itself. The outer loop updates the synthetic data $\mathcal S$ using a meta-gradient, computed by differentiating the matching loss with respect to $\mathcal S$. This requires backpropagating through the computation of the synthetic gradient $g_{\mathcal S}$, and therefore, through the GNN architecture

During this meta-gradient computation, the gradient of the loss with respect to a node's features is influenced by the gradients of its neighbors, causing the gradient to flow backward along the graph edges:

$$\nabla_{h_i^{(k-1)}} \mathcal{L} = \sum_{j|i \in \mathcal{N}(j)} \frac{\partial \mathcal{L}}{\partial h_j^{(k)}} \frac{\partial h_j^{(k)}}{\partial h_i^{(k-1)}}$$
 (5)

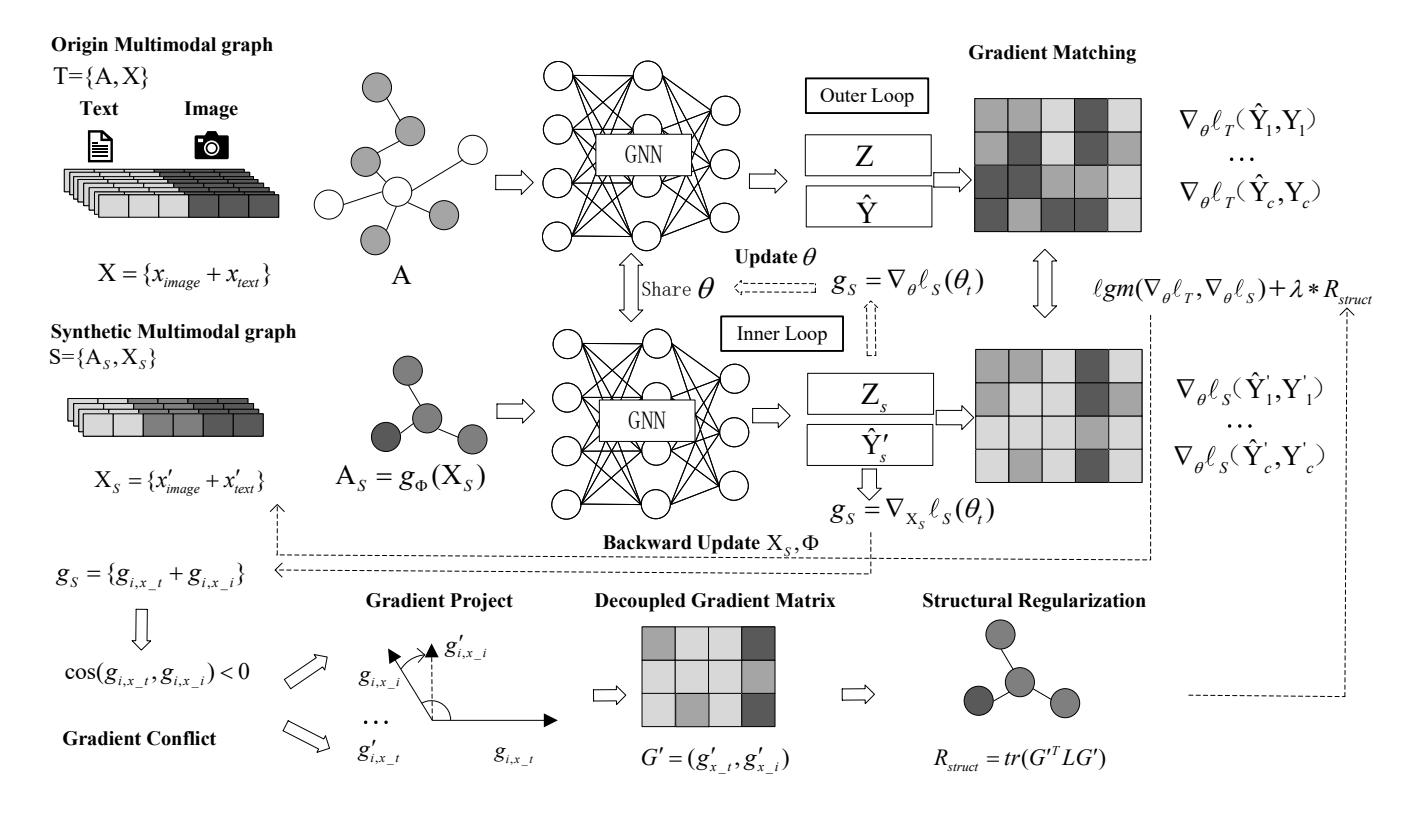


Figure 1: This is the overall framework of SR-GM. \mathcal{T} and \mathcal{S} denote the target and condensed multimodal graph datasets, respectively. The GNN is a graph neural network parameterized by θ . ℓ and ℓ_{gm} represent the task loss and the gradient matching loss function, respectively. $\nabla_{\theta}\ell_{\mathcal{S}}(\theta_t)$ denotes the gradient with respect to the model parameters θ , while $\nabla_{X_S}\ell_{\mathcal{S}}(\theta_t)$ denotes the gradient with respect to the synthetic node features X_s . g_{Φ} is an edge generator implemented by an MLP network, and the synthetic adjacency matrix A_s is generated by g_{Φ} taking X_s as input. Z and \hat{Y} represent the output features and predicted labels of the network, respectively.

This dynamic transforms the GNN's computational graph into a medium for noise propagation. The localized gradient conflicts at individual nodes are not contained; instead, they are amplified and propagated throughout the graph structure. This creates a highly non-smooth gradient field over the synthetic graph, where the optimization directions for adjacent nodes can be wildly different.

This structural amplification can be formally quantified using the Dirichlet Energy [53] of the feature gradient field. Let G_S be the $N' \times d$ matrix where each row is the feature gradient $\nabla_{\mathbf{X}_{S,i}} \mathcal{L}$ for a synthetic node i, and let \mathbf{L}_S be the graph Laplacian. The Dirichlet energy of the gradient field is:

$$E(G_{\mathcal{S}}) = \operatorname{tr}(G_{\mathcal{S}}^{T} \mathbf{L}_{\mathcal{S}} G_{\mathcal{S}})$$
(6)

$$= \frac{1}{2} \sum_{(i,j) \in E_{\mathcal{S}}} w_{ij} \| \nabla_{\mathbf{X}_{\mathcal{S},i}} \mathcal{L} - \nabla_{\mathbf{X}_{\mathcal{S},j}} \mathcal{L} \|_{2}^{2}$$
 (7)

A high Dirichlet energy signifies a chaotic gradient field. The structural amplification mechanism ensures this energy remains high, creating a rugged optimization landscape for $\mathcal S$ and causing the meta-gradient to be unstable. This persistent instability in the gradient field directly undermines the condensation objective, making it difficult to learn a small yet representative synthetic graph.

3.5 The Proposed SR-GM Framework

To address this dual challenge, as shown in Figure 1, we propose **Structurally-Regularized Gradient Matching (SR-GM)**, a framework that re-engineers the condensation process through two synergistic components: Gradient Decoupling and Structural Damping.

3.5.1 Parametrization of the Synthetic Graph. In SR-GM, the synthetic graph S is parameterized by its node features X_S and the parameters Φ of a structure generator network g_{Φ} . The node features X_S are learned directly. Following GCond [13], the adjacency matrix A_S is not directly parameterized but is generated as a function of the node features: $A_S = g_{\Phi}(X_S)$.

Specifically, the weight of an edge between nodes i and j is computed by a shared MLP, which is a multi-layer perceptron with parameters Φ :

$$(\mathbf{A}_{\mathcal{S}})_{ij} = \operatorname{Sigmoid}\left(\frac{\operatorname{MLP}_{\Phi}([\mathbf{x}_i; \mathbf{x}_j]) + \operatorname{MLP}_{\Phi}([\mathbf{x}_j; \mathbf{x}_i])}{2}\right) \quad (8)$$

where $[\cdot;\cdot]$ denotes concatenation. This formulation makes the graph structure differentiable with respect to both the node features X_S and the generator parameters Φ , and naturally enforces

symmetry for undirected graphs. The set of learnable parameters for the outer loop is thus $\{X_S, \Phi\}$.

3.5.2 Gradient Decoupling via Orthogonal Projection. To resolve the root cause of instability, we perform "gradient surgery" on the feature gradients [18, 46] of each synthetic node. This process is a prerequisite for computing the structural regularization term and is integrated into the outer loop's meta-gradient calculation.

Working Mechanism: At each inner-loop step t, after computing the synthetic loss $\mathcal{L}_{\mathcal{S}}(\theta_t)$, we first compute the gradient of this loss with respect to the synthetic features X_S . This yields the feature gradient matrix $G_S \in \mathbb{R}^{N' \times d}$:

$$G_{\mathcal{S}} = \nabla_{X_{\mathcal{S}}} \mathcal{L}_{\mathcal{S}}(\theta_t) \tag{9}$$

Since the synthetic features $\mathbf{X}_{\mathcal{S}}$ are a concatenation of modal features, the resulting gradient matrix G_S has the same structure. For each node s_i , we can partition its corresponding row vector in G_S to obtain the modality-specific gradients, $g_{i,\text{text}}$ and $g_{i,\text{image}}$.

If a conflict exists ($\langle g_{i,\text{text}}, g_{i,\text{image}} \rangle < 0$), we project each gradient onto the normal plane of the other to eliminate the conflicting components, following the PCGrad [46] methodology:

$$\mathbf{g'}_{i,\text{text}} = \mathbf{g}_{i,\text{text}} - \frac{\langle \mathbf{g}_{i,\text{text}}, \mathbf{g}_{i,\text{image}} \rangle}{\|\mathbf{g}_{i,\text{image}}\|^2} \mathbf{g}_{i,\text{image}}$$
(10)

$$g'_{i,\text{text}} = g_{i,\text{text}} - \frac{\langle g_{i,\text{text}}, g_{i,\text{image}} \rangle}{\|g_{i,\text{image}}\|^2} g_{i,\text{image}}$$
(10)
$$g'_{i,\text{image}} = g_{i,\text{image}} - \frac{\langle g_{i,\text{image}}, g_{i,\text{text}} \rangle}{\|g_{i,\text{text}}\|^2} g_{i,\text{text}}$$
(11)

This operation yields a decoupled feature gradient matrix G'_{S} , where each row is the reconciled gradient $g'_{i} = g'_{i,\text{text}} + g'_{i,\text{image}}$.

3.5.3 Structural Damping via Gradient Field Regularization. To counteract the structural amplification of noise, we introduce a novel regularization term that operates directly on the decoupled gradient field. Unlike traditional graph regularization [45] on node features, which GNNs already implicitly perform, our regularizer enforces smoothness on the optimization directions themselves. Let G's be the matrix of decoupled feature gradients from Equation (7). The structural regularization term is the Dirichlet energy of this gradient field:

$$\mathcal{R}_{\text{struct}}(G'_{S}) = \text{tr}(G'_{S}^{\top} L_{S} G'_{S}) = \sum_{(i,j) \in E_{S}} w_{ij} \|g'_{i} - g'_{j}\|^{2}$$
 (12)

This term penalizes large differences in optimization directions between connected nodes, forcing the gradient field to be smooth. It thereby transforms the graph structure from a "conflict amplifier" into an "optimization damper."

3.5.4 Final Objective and Algorithm. By integrating both components, the final SR-GM objective function becomes:

$$\min_{\mathcal{S}} \mathbb{E}_{\theta_t} \left[D(\nabla_{\theta} \mathcal{L}_{\mathcal{S}}(\theta_t), \nabla_{\theta} \mathcal{L}_{\mathcal{T}}(\theta_t)) + \lambda \cdot \mathcal{R}_{\text{struct}} \right]$$
(13)

where λ is a hyperparameter balancing gradient matching accuracy with gradient field smoothness. The gradient matching loss $\mathcal{L}_{gm} = D(\nabla_{\theta} \mathcal{L}_{\mathcal{S}}(\theta_t), \nabla_{\theta} \mathcal{L}_{\mathcal{T}}(\theta_t))$ follows the implementation in GCond [13]. SR-GM design fundamentally repurposes the graph structure from a source of instability into a tool for stabilization. The complete procedure, which correctly interleaves the outer-loop

update of S and the inner-loop update of θ , is detailed in Algorithm

```
Algorithm 1 Structure-Regularized Gradient Matching (SR-GM)
Require: Original graph \mathcal{T}, GNN model \phi_{\theta}, hyperparameters \lambda,
     \eta_S, \eta_{\Phi}, \eta_{\theta}, outer-loop iterations K, inner-loop iterations T
Ensure: Optimized synthetic features X_S and structure generator
  1: Initialize synthetic features \mathbf{X}_{\mathcal{S}} and g_{\Phi} parameters \Phi
  2: for k = 1 to K do
           Initialize GNN parameters \theta_0 \sim P_{\theta_0}
  4:
           \mathbf{for}\ t = 0\ \mathbf{to}\ T - 1\ \mathbf{do}
  5:
                Sample a batch \mathcal{T}' from \mathcal{T}
                Compute real data gradient \mathbf{g}_{\mathcal{T}} = \nabla_{\theta} \mathcal{L}_{\mathcal{T}'}(\theta_t)
  6:
                Generate synthetic adjacency matrix A_S = g_{\Phi}(X_S)
     using Eq. (8)
                Compute synthetic loss \mathcal{L}_{\mathcal{S}}(\theta_t) on \mathcal{S} = (\mathbf{X}_{\mathcal{S}}, \mathbf{A}_{\mathcal{S}})
  8:
                Compute synthetic model gradient \mathbf{g}_{\mathcal{S}} = \nabla_{\theta} \mathcal{L}_{\mathcal{S}}(\theta_t)
                Compute synthetic feature gradient matrix G_S =
 10:
      \nabla_{\mathbf{X}_{\mathcal{S}}} \mathcal{L}_{\mathcal{S}}(\theta_t)
     // Component I: Gradient Decoupling
                Construct decoupled gradient matrix G'_{\mathcal{S}} from G_{\mathcal{S}} us-
     ing Eq. (10) (11)
     // Component II: Structural Damping
                Compute structure regularization loss \mathcal{R}_{\text{struct}} using Eq.
 12:
     (12)
     // Meta-Update of Synthetic Data (Outer Loop)
 13:
                Compute gradient matching loss \mathcal{L}_{gm} = D(g_{\mathcal{S}}, g_{\mathcal{T}})
                Compute total update loss \mathcal{L}_{update} = \mathcal{L}_{gm} + \lambda \cdot \mathcal{R}_{struct}
                Update X_S, \Phi using \nabla_{X_S,\Phi} \mathcal{L}_{update} and learning rates
 15:
     \eta_{\mathcal{S}}, \eta_{\Phi}
     // Update Model Parameters (Inner Loop Curriculum
     Step)
                Update model parameters \theta_{t+1} \leftarrow \theta_t - \eta_\theta g_S
 16
 17:
 18: end for
```

Experiment

To empirically evaluate the effectiveness and generalization capability of our proposed SR-GM framework, we conducted a comprehensive set of experiments. This section is structured as follows: We begin by detailing the experimental setup, including datasets, evaluation protocols, and competing methods. Subsequently, we compare SR-GM against a series of representative baselines to demonstrate its superior performance. To further validate the robustness and architecture-agnostic nature of our framework, we then investigate its effectiveness when integrated with various GNN architectures. Furthermore, we perform experiments on SR-GM's training convergence and modality correlation, aiming to explore its training efficiency and the impact of inter-modal conflict on multimodal graph condensation. Finally, we conduct extensive experiments on key hyperparameters—specifically, the damping coefficient λ

19: **return** Optimized synthetic features X_S and generator param-

Table 1: Statistics of datasets.

Name	Nodes	Edges	Train/Val/Test
Ele-fashion	97,766	199,602	58,659/9,777/29,330
Goodreads-NC	685,294	7,235,084	406,689/67,805/203,428
Amazon-Sports	31,073	351,294	21,751/4,660/4,662
Amazon-Cloth	84,357	1,107,964	59,049/12,653/12,655

and the condensation ratio r—thereby providing a thorough validation of SR-GM's effectiveness on multimodal graph data. All the experiments are conducted on an NVIDIA RTX 3090 GPU.

4.1 Experimental Setup

Datasets. We evaluate the condensation performance of the proposed framework on 4 multimodal datasets, i.e., Ele-fashion [23] and Goodreads-NC [34] for inductive setting and Amazon-Sports, Amazon-Cloth for transductive setting. Following [1], we construct binary classification datasets for Amazon-Sports and Amazon-Cloth from the Amazon e-commerce platform¹; reviews with ratings \geq 4 are labeled as positive, and those with ratings < 2 as negative. Text and visual features for the Amazon-Sports and Amazon-Cloth datasets are encoded and aligned with ImageBind [10], while CLIP [25] is used for the Goodreads-NC and Ele-fashion datasets. The resulting features have dimensions of 1024 for Ele-fashion and Goodreads-NC, and 2048 for Amazon-Sports and Amazon-Cloth, and in all cases, the text and image modalities each constitute half of the total dimensionality. For the inductive setting, the test graph is not available during training. Dataset statistics are shown in Table 1.

Baselines. To demonstrate the effectiveness of SR-GM, we benchmark it against a comprehensive suite of baselines, which can be categorized into **coreset selection** and **graph condensation** methods. For **coreset selection**, we induce a subgraph from a representative node subset. We evaluate three selection strategies: **Random**, **Herding** [42], and **K-Center** [29]. For **graph condensation**, we employ three methods. **GCond** [13] and **MSGC** [8] aim to preserve performance by matching GNN training gradients. In contrast, **SGDD** [44] focus on maintaining global graph properties by preserving the graph's spectral characteristics and connectivity patterns.

Evaluation. We evaluate the quality of the condensed graphs by their ability to preserve performance on the downstream task of inductive node classification. For each baseline and our proposed SR-GM, we first generate a condensed graph containing rN nodes from the original training graph of N nodes, where $r \in (0,1)$ is the condensation ratio. The evaluation follows a two-stage protocol. In the **training stage**, a standard GNN model is trained exclusively on the small, condensed graph. Crucially, the original full graph is entirely discarded and inaccessible during this stage. In the subsequent **test stage**, the GNN model trained on the condensed graph is applied to the original, unseen test graph to perform inference on the test nodes. The primary metric for evaluation is the

resulting test accuracy. To ensure robust conclusions, we repeat all experiments 5 times and report the mean accuracy and its variance.

4.2 Comparison with Baselines

In this subsection, we test the performance of a 2-layer GCN on the condensed graphs, and compare the proposed SR-GM with baselines. Table 2 reports node classification performance. As shown in Table 2, our proposed SR-GM achieves performance that is comparable to, and often superior to, that of the baseline methods across all datasets and condensation ratios. We make the following observations:

Superiority of SR-GM. Our proposed SR-GM significantly outperforms most baseline methods across all datasets and condensation ratios. For instance, on the Goodreads-NC dataset at a 0.025% ratio, SR-GM achieves 66.43% accuracy, creating a substantial performance margin of nearly 9 percentage points over the strongest baseline, GCond.

Stability and Robustness. Beyond superior accuracy, SR-GM demonstrates exceptional stability, especially in settings where other methods falter. As seen in Table 2, GCond exhibit unstable performance on datasets like Ele-fashion. SGDD and MSGC even fail on Goodreads-NC. In stark contrast, SR-GM consistently produces high-performing condensed graphs with low variance across all runs. We attribute this robustness to our optimization objective, which is designed to mitigate the gradient conflict between different modalities.

Impact of condensation Ratio. As expected, the accuracy of most methods improves as the condensation ratio (r) increases, since a larger condensed graph can store more information. However, it is crucial to note that the performance gap between SR-GM and the baselines is most pronounced at lower condensation ratios. For example, on Ele-fashion, the accuracy improvement of SR-GM over the next-best baseline is larger at r=0.1% than at r=0.5%.

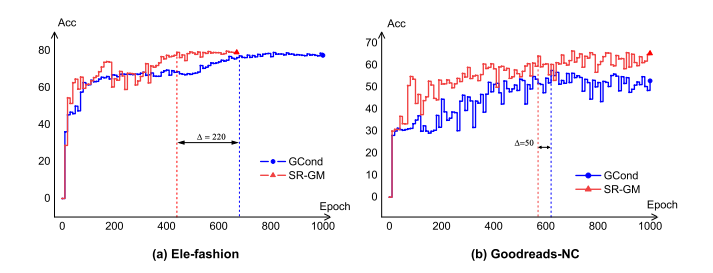


Figure 2: Comparison of condensation efficiency between our proposed SR-GM and the baseline GCond on the Elefashion and Goodreads-NC datasets. We can observe that SR-GM achieves comparable or superior peak performance to GCond with a faster convergence speed.

4.3 Condensation Efficiency

In this section, we empirically evaluate the condensation efficiency of SR-GM against GCond. This is achieved by analyzing the relationship between the performance of a node classification model and the number of training epochs spent optimizing the condensed

¹https://www.amazon.com/

Table 2: Inductive performance on Ele-fashion , Goodreads-NC and Transductive performance on Amazon-Sports, Amazon-Cloth. Performance is reported as test accuracy (%) for inductive and AUC score for transductive. "Original" denotes models trained on original graph. The best accuracies are bolded and the second best are underlined. \triangle (%) denotes the improvements of SR-GM upon the sub-optimal result.

			Proposed							
Dataset	Ratio (r)	Random	Herding	K-Center	MSGC	SGDD	GCond	SR-GM	△(%)	Original
	0.1%	63.28±0.25	64.17±0.16	65.59±0.21	68.71±0.82	71.08±0.08	78.93±0.06	79.85±0.22	↑0.92	
Ele-fashion	0.3%	68.48 ± 0.49	67.40 ± 0.50	68.82 ± 0.64	76.93 ± 0.37	75.68 ± 0.62	68.00 ± 0.78	82.03 ± 0.13	↑ 5.10	85.68±0.08
	0.5%	70.25 ± 0.24	67.41±0.14	70.37 ± 0.36	79.09±0.40	75.15 ± 0.11	71.42 ± 0.28	80.64 ± 0.17	↑1.55	
Goodreads-NC	0.025%	46.45±0.47	44.71±0.32	44.78±0.77	38.14±1.43	36.75±0.25	57.59±0.55	66.43±0.60	↑8.84	70.45 . 0.04
Goodreads-NC	0.05%	47.60 ± 0.27	44.73 ± 0.36	44.82±0.35	43.10 ± 0.23	31.68 ± 1.27	58.09±0.66	$68.20 \!\pm\! 0.31$	↑10.11	79.45±0.04
	0.1%	61.14±0.14	61.13±0.15	62.10±0.20	65.43±0.53	63.52±0.70	64.14±0.53	67.78±0.52	↑2.35	
Amazon-Sports	0.3%	59.23 ± 0.63	61.51±0.07	61.76±0.58	65.07 ± 0.53	63.07 ± 0.42	64.86 ± 0.75	70.25 ± 0.55	↑ 5.18	70.50 ± 0.47
•	0.5%	60.37 ± 0.25	61.76±0.25	64.31±0.24	67.90±0.12	65.56 ± 0.42	65.28 ± 0.47	71.12 ± 0.70	↑3.22	
	0.1%	52.49±0.01	50.82±0.15	51.11±0.20	57.80±0.30	58.30±0.49	57.46±0.57	65.96±0.44	↑7.66	
Amazon-Cloth	0.3%	54.85 ± 0.46	53.31±0.35	57.26 ± 0.48	65.88 ± 0.22	61.47±0.07	58.32±0.67	66.87 ± 0.30	↑0.99	71.59 ± 0.27
	0.5%	52.92 ± 0.23	54.54 ± 0.50	53.75 ± 0.36	64.97±0.14	61.37 ± 0.48	57.88±0.99	67.64 ± 0.14	1 2.67	

dataset. Figure 2 illustrates this relationship, with each curve representing the performance trajectory and terminating upon reaching its peak.

As shown in Figure 2, SR-GM converges faster by 220 and 50 epochs on the Ele-fashion and Goodreads-NC datasets, respectively. Results demonstrates that SR-GM performances on par with, or even superior to GCond while maintaining a comparable convergence speed.

Table 3: Evaluation of cross-architecture generalizability. Test accuracy (%) of various GNN architectures trained on a graph condensed by SR-GM (with a GCN backbone).SAGE stands for GraphSAGE. Avg. stands for the average test accuracy.

Dataset	Methods	GCN	MLP	MMGCN	GAT	SAGE	Avg.
Ele-fashion $r = 0.1\%$				71.53 75.88			
Goodreads-NC $r = 0.05\%$						53.56 64.16	

4.4 Cross-Architecture Generalizability

To evaluate the cross-architecture generalizability of our method, we condense a graph using SR-GM with a GCN backbone and then use this single condensed graph to train several different GNN architectures. As reported in Table 3, we test a diverse set of models, including GraphSAGE [11], GAT [33], a multimodal GNN (MMGCN) [41], and a simple MLP [32]. The performance across these varied architectures demonstrates that the graphs condensed by SR-GM are not overfitted to the condensation model and possess good generalization capabilities.

Table 4: Test accuracy (%) of SR-GM on the Ele-fashion datasets when using different backbone models for both condensation and evaluation. SAGE is an abbreviation for Graph-SAGE. Original means training on original graph.

Backbone	Ratio (r)	SR-GM	GCond	Original
GCN	0.1% 0.5%	79.85±0.22 80.64±0.17	78.93±0.06 71.42±0.28	85.68±0.08
SAGE	0.1% 0.5%	81.20±0.09 82.66±0.21	80.17±0.58 82.08±0.24	87.52±0.01
MLP	0.1% 0.5%	77.27±0.34 78.95±0.38	77.07±0.51 78.28±0.52	88.37±0.03

4.5 Architectural Agnosticism of SR-GM

A key advantage of our SR-GM framework is its architectural agnosticism, meaning it is not tightly coupled to a specific GNN architecture. To demonstrate this flexibility, we conducted an experiment where we varied the underlying graph neural network used within the SR-GM condensation process.

We selected a diverse set of models for this evaluation, including popular GNNs such as GCN and GraphSAGE. Crucially, we also included a standard MLP as a stress test. The MLP is entirely graphagnostic and processes only node features, allowing us to evaluate SR-GM's ability to condense structural information even when the internal model does not perform message passing.

As shown in Table 4, we report the performance on the Elefashion dataset, where for each run, the same model (e.g., GCN) was used for both condensation and downstream evaluation. The results compellingly show that SR-GM consistently yields highly effective condensed graphs across all tested architectures, including the MLP. This strongly validates our claim that SR-GM's effectiveness is not contingent on a particular GNN backbone, highlighting its robustness and wide applicability.

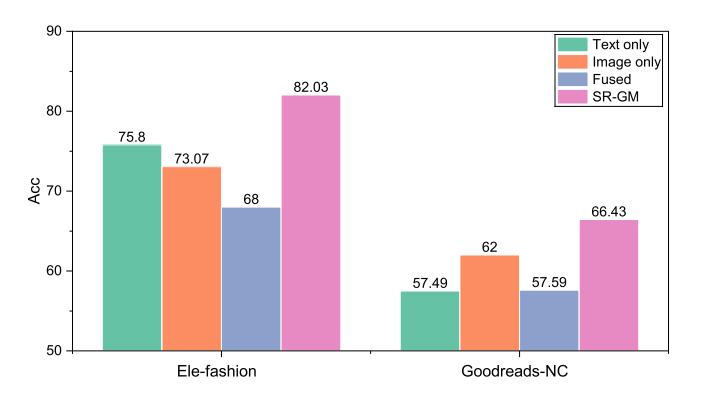


Figure 3: Test accuracy (%) for SR-GM and GC ond using different input features: text-only, image-only, and fused text-image features on Ele-fashion and Goodreads-NC.

4.6 Ablation Study on the Impact of Multimodal Features

To investigate the impact of multimodal features on the performance of graph condensation, we conduct a comprehensive ablation study. In this experiment, we apply the baseline GCond method to graphs constructed with three different types of input features: text-only, image-only, and fused text-image features. We then compare its performance against our proposed SR-GM, which is implemented within the GCond framework to specifically address multimodal challenges. The node classification test accuracy on the Ele-fashion and Goodreads-NC datasets for these configurations is presented in Figure 3.

As illustrated in the figure, the introduction of fused multimodal data adversely affects the standard GCond method. We observe that the inherent conflict between different modalities leads to an average performance degradation of approximately 6% for GCond when compared to its performance on single-modality inputs. This highlights a significant challenge for existing gradient-matching-based condensation methods when applied to multimodal graphs. In contrast, our proposed SR-GM successfully mitigates this intermodality gradient conflict during the condensation process. Consequently, SR-GM significantly outperforms GCond on the multimodal graph condensation task, achieving substantial accuracy improvements of 14% on Ele-fashion and 9% on Goodreads-NC. This result underscores the robustness and effectiveness of SR-GM in handling complex, multimodal graph data.

4.7 Parameter Analysis of Regularization Weight λ

A critical hyperparameter in SR-GM is the regularization weight, denoted by λ , which significantly influences the model's performance. To investigate its impact on the graph condensation process, we conduct experiments on the Ele-fashion dataset under various settings of λ and condensation ratio (r). The resulting test accuracies are visualized in a heatmap, as illustrated in Figure 4, where darker shades indicate higher accuracy.

From the results, we draw two primary observations. First, SR-GM demonstrates robust performance across most configurations,

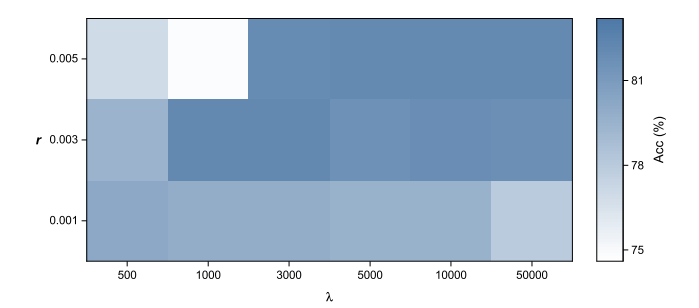


Figure 4: Heatmap of test accuracy for SR-GM on the Elefashion dataset under different settings of condensation rate (r) and regularization weight (λ). Darker shades correspond to higher accuracy, indicating better performance.

achieving high accuracy on the Ele-fashion dataset. A notable exception occurs at r of 0.05%, where performance degrades for λ values of 500 and 1000. Second, the findings suggest that while SR-GM is largely insensitive to high values of λ , an important correlation exists between r and λ . Specifically, as r increases (i.e., the number of nodes in the condensed graph grows), a correspondingly larger λ is required to maintain optimal performance and prevent a significant decline in accuracy.

5 Conclusion

In this paper, we identify two fundamental challenges leading to the failure of current multimodal graph condensation methods: gradient conflicts arising from synthetic node features and the pathological amplification of gradient noise by graph structures. To address these issues, we propose a novel framework, Structurally-Regularized Gradient Matching (SR-GM), for condensing multimodal graph data. Specifically, SR-GM tackles the problem through a bi-level optimization formulation that incorporates two synergistic components. First, a gradient disentanglement mechanism resolves inter-modal conflicts at their source via orthogonal projection. Second, a structural damping regularizer, based on the Dirichlet energy of the gradient field, transforms the graph topology from a noise amplifier into an optimization stabilizer. Experimental results demonstrate the superiority of the proposed SR-GM in both efficiency and effectiveness. Furthermore, SR-GM exhibits strong generalization capabilities across various GNN architectures on multimodal graph-structured data.

References

- Jie Cai, Xin Wang, Haoyang Li, Ziwei Zhang, and Wenwu Zhu. 2024. Multimodal graph neural architecture search under distribution shifts. In Proceedings of the AAAI Conference on Artificial Intelligence, Vol. 38. 8227–8235.
- [2] Heyan Chai, Zeyu Liu, Yongxin Tong, Ziyi Yao, Binxing Fang, and Qing Liao. 2024. Towards task-conflicts momentum-calibrated approach for multi-task learning. In 2024 IEEE 40th International Conference on Data Engineering (ICDE). IEEE, 939–952.
- [3] Shumin Deng, Chengming Wang, Zhoubo Li, Ningyu Zhang, Zelin Dai, Hehong Chen, Feiyu Xiong, Ming Yan, Qiang Chen, Mosha Chen, et al. 2023. Construction and applications of billion-scale pre-trained multimodal business knowledge graph. In 2023 IEEE 39th International Conference on Data Engineering (ICDE). IEEE 2088 2002
- [4] Alexey Dosovitskiy. 2020. An image is worth 16x16 words: Transformers for image recognition at scale. arXiv preprint arXiv:2010.11929 (2020).

- [5] Junfeng Fang, Xinglin Li, Yongduo Sui, Yuan Gao, Guibin Zhang, Kun Wang, Xiang Wang, and Xiangnan He. 2024. Exgc: Bridging efficiency and explainability in graph condensation. In Proceedings of the ACM Web Conference 2024. 721–732.
- [6] Duoduo Feng, Xiangteng He, and Yuxin Peng. 2023. MKVSE: Multimodal knowledge enhanced visual-semantic embedding for image-text retrieval. ACM Transactions on Multimedia Computing, Communications and Applications 19, 5 (2023), 1–21.
- [7] Jiarui Feng, Yixin Chen, Fuhai Li, Anindya Sarkar, and Muhan Zhang. 2022. How powerful are k-hop message passing graph neural networks. Advances in Neural Information Processing Systems 35 (2022), 4776–4790.
- [8] Jian Gao and Jianshe Wu. 2023. Multiple sparse graphs condensation. Knowledge-Based Systems 278 (2023), 110904.
- [9] Jian Gao, Jianshe Wu, and Jingyi Ding. 2024. Heterogeneous graph condensation. IEEE Transactions on Knowledge and Data Engineering 36, 7 (2024), 3126–3138.
- [10] Rohit Girdhar, Alaaeldin El-Nouby, Zhuang Liu, Mannat Singh, Kalyan Vasudev Alwala, Armand Joulin, and Ishan Misra. 2023. Imagebind: One embedding space to bind them all. In Proceedings of the IEEE/CVF conference on computer vision and pattern recognition. 15180–15190.
- [11] Will Hamilton, Zhitao Ying, and Jure Leskovec. 2017. Inductive representation learning on large graphs. Advances in neural information processing systems 30 (2017).
- [12] Wei Jin, Xianfeng Tang, Haoming Jiang, Zheng Li, Danqing Zhang, Jiliang Tang, and Bing Yin. 2022. Condensing graphs via one-step gradient matching. In Proceedings of the 28th ACM SIGKDD Conference on Knowledge Discovery and Data Mining. 720–730.
- [13] Wei Jin, Lingxiao Zhao, Shichang Zhang, Yozen Liu, Jiliang Tang, and Neil Shah. 2021. Graph condensation for graph neural networks. arXiv preprint arXiv:2110.07580 (2021).
- [14] Dhruv Khattar, Jaipal Singh Goud, Manish Gupta, and Vasudeva Varma. 2019. Mvae: Multimodal variational autoencoder for fake news detection. In *The world wide web conference*. 2915–2921.
- [15] TN Kipf. 2016. Semi-supervised classification with graph convolutional networks. arXiv preprint arXiv:1609.02907 (2016).
- [16] Rong Li, Long Xu, Songbai Liu, Junkai Ji, Lingjie Li, Qiuzhen Lin, and Lijia Ma. 2025. Structure Balance and Gradient Matching-Based Signed Graph Condensation. In Proceedings of the AAAI Conference on Artificial Intelligence, Vol. 39. 12121–12129.
- [17] Victor Weixin Liang, Yuhui Zhang, Yongchan Kwon, Serena Yeung, and James Y Zou. 2022. Mind the gap: Understanding the modality gap in multi-modal contrastive representation learning. Advances in Neural Information Processing Systems 35 (2022), 17612–17625.
- [18] Bo Liu, Xingchao Liu, Xiaojie Jin, Peter Stone, and Qiang Liu. 2021. Conflict-averse gradient descent for multi-task learning. Advances in Neural Information Processing Systems 34 (2021), 18878–18890.
- [19] Mengyang Liu, Shanchuan Li, Xinshi Chen, and Le Song. 2022. Graph condensation via receptive field distribution matching. arXiv preprint arXiv:2206.13697 (2022).
- [20] Yaxin Liu, Yan Zhou, Ziming Li, Jinchuan Zhang, Yu Shang, Chenyang Zhang, and Songlin Hu. 2024. Rng: reducing multi-level noise and multi-grained semantic gap for joint multimodal aspect-sentiment analysis. In 2024 IEEE International Conference on Multimedia and Expo (ICME). IEEE, 1–6.
- [21] Pingchuan Ma, Tao Du, and Wojciech Matusik. 2020. Efficient continuous pareto exploration in multi-task learning. In *International Conference on Machine Learn*ing. PMLR, 6522–6531.
- [22] Debabrata Mahapatra and Vaibhav Rajan. 2020. Multi-task learning with user preferences: Gradient descent with controlled ascent in pareto optimization. In International Conference on Machine Learning. PMLR, 6597–6607.
- [23] Jianmo Ni, Jiacheng Li, and Julian McAuley. 2019. Justifying recommendations using distantly-labeled reviews and fine-grained aspects. In Proceedings of the 2019 conference on empirical methods in natural language processing and the 9th international joint conference on natural language processing (EMNLP-IJCNLP). 188–197.
- [24] Xuying Ning, Dongqi Fu, Tianxin Wei, Wujiang Xu, and Jingrui He. 2025. Graph4MM: Weaving Multimodal Learning with Structural Information. In Forty-second International Conference on Machine Learning.
- [25] Alec Radford, Jong Wook Kim, Chris Hallacy, Aditya Ramesh, Gabriel Goh, Sandhini Agarwal, Girish Sastry, Amanda Askell, Pamela Mishkin, Jack Clark, et al. 2021. Learning transferable visual models from natural language supervision. In International conference on machine learning. PmLR, 8748–8763.
- [26] Colin Raffel, Noam Shazeer, Adam Roberts, Katherine Lee, Sharan Narang, Michael Matena, Yanqi Zhou, Wei Li, and Peter J Liu. 2020. Exploring the limits of transfer learning with a unified text-to-text transformer. *Journal of machine* learning research 21, 140 (2020), 1–67.
- [27] Yu Rong, Wenbing Huang, Tingyang Xu, and Junzhou Huang. 2019. Dropedge: Towards deep graph convolutional networks on node classification. arXiv preprint arXiv:1907.10903 (2019).
- [28] Tara Safavi and Danai Koutra. 2020. CoDEx: A Comprehensive Knowledge Graph Completion Benchmark. In Proceedings of the 2020 Conference on Empirical

- $Methods\ in\ Natural\ Language\ Processing\ (EMNLP).\ 8328-8350.$
- [29] Ozan Sener and Silvio Savarese. 2017. Active learning for convolutional neural networks: A core-set approach. arXiv preprint arXiv:1708.00489 (2017).
- [30] Yixin Su, Rui Zhang, Sarah Erfani, and Zhenghua Xu. 2021. Detecting beneficial feature interactions for recommender systems. In Proceedings of the AAAI conference on artificial intelligence, Vol. 35. 4357–4365.
- [31] Zhulin Tao, Yinwei Wei, Xiang Wang, Xiangnan He, Xianglin Huang, and Tat-Seng Chua. 2020. Mgat: Multimodal graph attention network for recommendation. Information Processing & Management 57, 5 (2020), 102277.
- [32] Hind Taud and Jean-Franccois Mas. 2017. Multilayer perceptron (MLP). In Geomatic approaches for modeling land change scenarios. 451–455.
- [33] Petar Velickovic, Guillem Cucurull, Arantxa Casanova, Adriana Romero, Pietro Lio, Yoshua Bengio, et al. 2017. Graph attention networks. stat 1050, 20 (2017), 10–48550
- [34] Mengting Wan and Julian McAuley. 2018. Item recommendation on monotonic behavior chains. In Proceedings of the 12th ACM conference on recommender systems. 86–94.
- [35] Xinchen Wan, Kaiqiang Xu, Xudong Liao, Yilun Jin, Kai Chen, and Xin Jin. 2023. Scalable and efficient full-graph gnn training for large graphs. Proceedings of the ACM on Management of Data 1, 2 (2023), 1–23.
- [36] Kai Wang, Bo Zhao, Xiangyu Peng, Zheng Zhu, Shuo Yang, Shuo Wang, Guan Huang, Hakan Bilen, Xinchao Wang, and Yang You. 2022. Cafe: Learning to condense dataset by aligning features. In Proceedings of the IEEE/CVF Conference on Computer Vision and Pattern Recognition. 12196–12205.
- [37] Lin Wang, Wenqi Fan, Jiatong Li, Yao Ma, and Qing Li. 2024. Fast graph condensation with structure-based neural tangent kernel. In Proceedings of the ACM Web Conference 2024. 4439–4448.
- [38] Meng Wang, Hao Li, Dacheng Tao, Ke Lu, and Xindong Wu. 2012. Multimodal graph-based reranking for web image search. IEEE transactions on image processing 21, 11 (2012), 4649–4661.
- [39] Tongzhou Wang, Jun-Yan Zhu, Antonio Torralba, and Alexei A Efros. 2018. Dataset distillation. arXiv preprint arXiv:1811.10959 (2018).
- [40] Zirui Wang, Yulia Tsvetkov, Orhan Firat, and Yuan Cao. 2020. Gradient vaccine: Investigating and improving multi-task optimization in massively multilingual models. arXiv preprint arXiv:2010.05874 (2020).
- [41] Yinwei Wei, Xiang Wang, Liqiang Nie, Xiangnan He, Richang Hong, and Tat-Seng Chua. 2019. MMGCN: Multi-modal graph convolution network for personalized recommendation of micro-video. In Proceedings of the 27th ACM international conference on multimedia. 1437–1445.
- [42] Max Welling. 2009. Herding dynamical weights to learn. In Proceedings of the 26th annual international conference on machine learning. 1121–1128.
- [43] Da Xu, Chuanwei Ruan, Evren Korpeoglu, Sushant Kumar, and Kannan Achan. 2020. Product knowledge graph embedding for e-commerce. In Proceedings of the 13th international conference on web search and data mining. 672–680.
- [44] Beining Yang, Kai Wang, Qingyun Sun, Cheng Ji, Xingcheng Fu, Hao Tang, Yang You, and Jianxin Li. 2023. Does graph distillation see like vision dataset counterpart? Advances in Neural Information Processing Systems 36 (2023), 53201– 53226.
- [45] Han Yang, Kaili Ma, and James Cheng. 2021. Rethinking graph regularization for graph neural networks. In Proceedings of the AAAI Conference on Artificial Intelligence, Vol. 35. 4573–4581.
- [46] Tianhe Yu, Saurabh Kumar, Abhishek Gupta, Sergey Levine, Karol Hausman, and Chelsea Finn. 2020. Gradient surgery for multi-task learning. Advances in neural information processing systems 33 (2020), 5824–5836.
- [47] Muhan Zhang and Yixin Chen. 2018. Link prediction based on graph neural networks. Advances in neural information processing systems 31 (2018).
- [48] Xin Zhang, Ziruo Zhang, Jiawei Du, Zuozhu Liu, and Joey Tianyi Zhou. 2025. Beyond Modality Collapse: Representations Blending for Multimodal Dataset Distillation. arXiv preprint arXiv:2505.14705 (2025).
- [49] Yongqi Zhang, Zhanke Zhou, Quanming Yao, and Yong Li. 2022. Efficient hyper-parameter search for knowledge graph embedding. In Proceedings of the 60th Annual Meeting of the Association for Computational Linguistics (Volume 1: Long Papers). 2715–2735.
- [50] Bo Zhao and Hakan Bilen. 2023. Dataset condensation with distribution matching. In Proceedings of the IEEE/CVF Winter Conference on Applications of Computer Vision 6514–6523
- [51] Bo Zhao, Konda Reddy Mopuri, and Hakan Bilen. 2020. Dataset condensation with gradient matching. arXiv preprint arXiv:2006.05929 (2020).
- [52] Xin Zheng, Miao Zhang, Chunyang Chen, Quoc Viet Hung Nguyen, Xingquan Zhu, and Shirui Pan. 2023. Structure-free graph condensation: From large-scale graphs to condensed graph-free data. Advances in Neural Information Processing Systems 36 (2023), 6026–6047.
- [53] Kaixiong Zhou, Xiao Huang, Daochen Zha, Rui Chen, Li Li, Soo-Hyun Choi, and Xia Hu. 2021. Dirichlet energy constrained learning for deep graph neural networks. Advances in neural information processing systems 34 (2021), 21834– 21846.
- [54] Jing Zhu, Yuhang Zhou, Shengyi Qian, Zhongmou He, Tong Zhao, Neil Shah, and Danai Koutra. 2025. Mosaic of modalities: A comprehensive benchmark for

multimodal graph learning. In Proceedings of the Computer Vision and Pattern Recognition Conference. 14215-14224.

A APPENDIX

A.1 Analysis of Feature Alignment Effects on Multimodal Graph Condensation

We conduct multimodal graph condensation experiments with unaligned feature encoding to simulate real-world scenarios with feature inconsistency, where textual features are encoded using T5 [26] (512-dimensional) and visual features using ViT [4] (512-dimensional). This heterogeneous encoding creates semantic gaps in the feature space, providing a challenging environment to validate SR-GM's robustness. As shown in Table 5, SR-GM maintains superior performance across all datasets and condensation ratios under unaligned conditions, achieving improvements of 7.81% over the sub-optimal method on Goodreads-NC at 0.05% condensation ratio and 3.11% on Amazon-Sports at 0.3% condensation ratio, confirming the effectiveness of gradient decoupling in mitigating multimodal gradient conflicts.

Comparative analysis between Table 2 (aligned features) and Table 5 (unaligned features) reveals that aligned conditions yield higher original dataset accuracy, with Ele-fashion achieving 85.68% versus 84.47%, Goodreads-NC reaching 79.45% versus 76.93%, and Amazon-Cloth attaining 71.59% versus 68.31%, reinforcing the crucial role of feature alignment in multimodal graph learning. However, the radar charts in Figure 5 demonstrate SR-GM's distinctive advantage: in both aligned and unaligned scenarios, it exhibits the smallest performance gap relative to original datasets, with Figure 5 particularly showing significantly smaller performance degradation compared to other condensation algorithms under unaligned conditions.

These findings highlight SR-GM's unique capability to maintain excellent performance in unaligned environments through its innovative gradient decoupling and structural regularization mechanisms, substantially reducing dependency on perfect feature alignment. This strong adaptability to unaligned feature environments positions SR-GM as a powerful solution for practical multimodal graph condensation challenges, especially considering that achieving perfect feature alignment in real-world applications is often prohibitively expensive or practically infeasible.

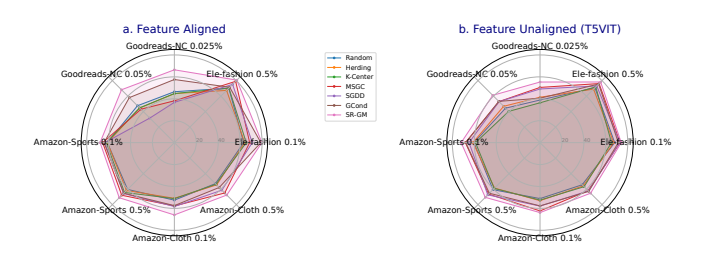


Figure 5: Average performance comparison between feature aligned and feature misaligned

A.2 Ablation Study on Gradient Decoupling and Structure Regularization

The ablation study results fully validate the effectiveness of the SR-GM framework in addressing gradient conflict issues in multimodal graph condensation. In feature-aligned CLIP encoding scenarios, structure regularization (R) demonstrates significant advantages, particularly on the Goodreads-NC dataset where the Δ_2 increments reach +7.56 to +8.88. This confirms our theoretical hypothesis regarding "structural damping" - by constraining the gradient field through Laplacian regularization, it effectively suppresses the propagation and amplification of local gradient conflicts within the graph structure. However, in high condensation ratio scenarios on the Ele-fashion dataset, the method relying solely on structure regularization ($\Delta_1 = -1.18$) shows limitations, reflecting that in feature-aligned and data-sufficient environments, structural constraints alone may be insufficient to completely resolve the deep optimization problems caused by inter-modal semantic gaps.

In contrast, the core value of gradient decoupling (D) becomes prominent in feature-unaligned T5VIT encoding environments. The stable Δ_1 increments of +2.58 to +4.00 on the Ele-fashion dataset directly confirm the crucial role of the gradient decoupling mechanism in handling conflicts among multimodal gradient signals. Particularly noteworthy is the negative Δ_2 increment observed for structure regularization under T5VIT encoding, a phenomenon that profoundly reveals how traditional structural constraints might instead reinforce incorrect gradient propagation paths in feature-unaligned environments. Gradient decoupling, through orthogonal projection to eliminate inter-modal gradient contradictions, provides a cleaner optimization foundation for structure regularization.

These findings strongly support the dual-design philosophy of SR-GM: gradient decoupling resolves multimodal gradient conflicts at their source, while structure regularization suppresses conflict amplification along propagation paths. The synergistic effect of these two components enables SR-GM to maintain robust performance across diverse multimodal graph scenarios, providing reliable technical support for practical applications of multimodal graph condensation.

Table 5: Inductive performance on Ele-fashion, Goodreads-NC and Transductive performance on Amazon-Sports, Amazon-Cloth using T5VIT encoding. Performance is reported as test accuracy (%) for inductive and AUC score for transductive. "Original" denotes models trained on original graph. The best accuracies are bolded and the second best are underlined. \triangle (%) denotes the improvements of SR-GM upon the sub-optimal result.

		Baselines						Proposed		
Dataset	Ratio (r)	Random	Herding	K-Center	MSGC	SGDD	GCond	SR-GM	△(%)	Original
	0.1%	68.09±0.81	67.23±0.30	65.25±0.35	73.03±0.11	72.85±0.14	71.44±0.22	74.09±0.13	↑1.06	
Ele-fashion	0.3%	72.22 ± 0.18	70.77 ± 0.34	70.26 ± 0.21	77.28 ± 0.08	72.75 ± 0.33	75.21 ± 0.11	77.47 ± 0.14	↑0.19	84.47 ± 0.05
	0.5%	70.83±0.79	69.07±0.54	71.93 ± 0.50	76.19±0.22	73.18 ± 0.45	75.59 ± 0.25	78.23 ± 0.13	^ 2.04	
Goodreads-NC	0.025%	38.86±1.07	41.43±0.70	36.34±0.78	50.37±0.42	48.95±1.08	40.53±0.30	55.28±0.11	↑4.91	76.93±0.02
Goodreads-NC	0.05%	44.48 ± 0.01	46.91±0.92	40.35 ± 0.54	52.95±0.15	52.87±0.29	53.22 ± 0.18	61.03 ± 0.21	↑ 7.81	70.93±0.02
	0.1%	60.29±0.08	61.22±0.16	58.86±0.16	68.06±0.08	64.79±0.11	67.87±0.19	71.95±0.18	↑3.89	
Amazon-Sports	0.3%	59.00 ± 0.17	60.56 ± 0.13	57.37 ± 0.37	68.21±0.19	66.32 ± 0.25	65.36 ± 0.31	71.32 ± 0.38	↑3.11	75.47 ± 0.20
	0.5%	60.70 ± 0.15	58.67 ± 0.28	59.11±0.39	66.38 ± 0.49	67.42 ± 0.58	65.32 ± 0.31	70.63 ± 0.31	↑3.21	
	0.1%	51.06±0.09	52.98±0.18	52.44±0.23	62.32±0.12	57.91±0.09	57.70±0.14	63.84±0.12	↑1.52	
Amazon-Cloth	0.3%	52.62 ± 0.60	54.95±0.39	55.21 ± 0.33	62.49 ± 0.06	60.96 ± 0.21	59.85 ± 0.08	65.61 ± 0.17	↑3.12	68.31 ± 0.10
	0.5%	54.38 ± 0.53	55.78 ± 0.34	56.86 ± 0.35	62.00±0.03	62.37 ± 0.06	62.89 ± 0.33	65.26 ± 0.14	↑ 2.37	

Table 6: SR-GM Ablation Study Results. D: gradient decoupling, R: structure regularization. Δ_1 : (SR-GM w/o D), Δ_2 : (SR-GM w/o D) - (SR-GM w/o D+R).

Dataset	Ratio (r)	Method	CLIP (Aligned)	T5VIT (Unaligned)	CLIP Increments	T5VIT Increments
		SR-GM	66.43±0.60	55.28±0.11	-	-
	0.025%	w/o D	65.15 ± 0.66	54.34±0.32	Δ_1 : +1.28	Δ_1 : +0.94
Goodreads-NC		w/o D+R	57.59±0.55	40.53 ± 0.30	Δ_2 : +7.56	Δ_2 : +13.81
Goodicads Ive		SR-GM	68.20±0.31	61.03±0.21	-	-
	0.05%	w/o D	66.97 ± 0.23	60.89±0.20	Δ_1 : +1.23	Δ_1 : +0.14
		w/o D+R	58.09 ± 0.66	53.22 ± 0.18	Δ_2 : +8.88	Δ_2 : +7.67
	0.1%	SR-GM	79.85±0.22	74.09±0.13	-	-
		w/o D	79.63 ± 0.27	71.09 ± 0.48	Δ_1 : +0.22	Δ_1 : +3.00
		w/o D+R	78.93 ± 0.06	71.44 ± 0.22	Δ_2 : +0.92	Δ_2 : -0.35
T1 C 1:		SR-GM	82.03±0.13	77.47±0.14	-	-
Ele-fashion	0.3%	w/o D	81.95±0.06	73.47 ± 0.07	Δ_1 : +0.08	Δ_1 : +4.00
		w/o D+R	68.00 ± 0.78	76.91 ± 0.11	Δ_2 : +13.95	Δ_2 : -3.44
		SR-GM	80.64±0.17	78.23±0.13	-	-
	0.5%	w/o D	81.82±0.25	75.65±0.25	Δ_1 : -1.18	Δ_1 : +2.58
		w/o D+R	71.42±0.28	78.55±0.07	Δ_2 : +10.40	Δ ₂ : -2.90